



ELSEVIER

Contents lists available at ScienceDirect

Data in Brief

journal homepage: www.elsevier.com/locate/dib

Data Article

Structural data of lanthanide complex constructed by 4-iodo-3-methyl benzoic acid and 4,7-dimethyl-1,10-phenanthroline



Yongli Zhao*, Ting Tang, Qingrong Yang, Ziqi Liu

College of Chemistry and Chemical Engineering, Key Laboratory of Functional Small Organic Molecule, Ministry of Education and Jiangxi's Key Laboratory of Green Chemistry, Jiangxi Normal University, Nanchang 330022, PR China

ARTICLE INFO

Article history:

Received 18 August 2018

Received in revised form

19 September 2018

Accepted 24 September 2018

ABSTRACT

In this data article, we present the FT-IR and PXRD data of the lanthanide complexes constructed by 4-iodo-3-methylbenzoic acid (IMBA) and 4,7-dimethyl-1,10-phenanthroline (dmp). Detailed structure analysis, luminescence and sensing properties were discussed in our previous study, "Highly Luminescent Lanthanide Complexes as Bifunctional Sensor for Et₂O and Fe²⁺" (Zhao et al., 2018). Also, the data include the bond lengths and angles of [Ln₂(IMBA)₆(dmp)₂] (Ln = Eu³⁺, **1a**; Ln = Gd³⁺, **1b**; Ln = Tb³⁺, **1c**).

© 2018 The Authors. Published by Elsevier Inc. This is an open access article under the CC BY license

(<http://creativecommons.org/licenses/by/4.0/>).

Specifications table

Subject area	Chemistry
More specific subject area	FT-IR, PXRD, structural bond lengths, angles data of lanthanide complexes
Type of data	Table, figure
How data was acquired	Crystallography open data base and crystallographic tool – Diamond: Crystallographic Information File Code: 1852307–1852309.cif
Data format	Analyzed

DOI of original article: <https://doi.org/10.1016/j.jlumin.2018.08.052>

* Corresponding author.

E-mail address: HNzhaoyongli@jxnu.edu.cn (Y. Zhao).

<https://doi.org/10.1016/j.dib.2018.09.063>

2352-3409/© 2018 The Authors. Published by Elsevier Inc. This is an open access article under the CC BY license (<http://creativecommons.org/licenses/by/4.0/>).

Experimental factors	Single crystal X-ray diffraction (SCXRD) data was collected on a Bruker SMART 1000 CCD at 298(2) K, with Mo-K α radiation (0.71073 \AA) at room temperature. The structure was refined by full-matrix least-squares methods with SHELXL-97 module. These single crystals are isostructural and they crystallize in triclinic space group P-1 (no. 2).
Experimental features	Block or needle-like colorless single crystal.
Data source location	Jiangxi Normal University, Nanchang, China.
Data accessibility	The data are with this article.
Related research article	Li-Wen Ding, Zi-Qi Liu, Highly Luminescent Lanthanide Complexes Constructed by Bis-tridentate Ligand and as Sensor for Et ₂ O, submitted.

Value of the data

- This structure information would be valuable for FT-IR analysis of lanthanide complexes.
- This data would be worthy for further investigation of the PXRD properties.
- This data provide a new process to synthesize two ligands coordinated lanthanide complexes.

1. Data

The single crystal structures of $[\text{Ln}_2(\text{IMBA})_6(\text{dmp})_2]$ ($\text{Ln}=\text{Eu}^{3+}$, **1a**; $\text{Ln}=\text{Gd}^{3+}$, **1b**; $\text{Ln}=\text{Tb}^{3+}$, **1c**) are isostructural. They crystallize in triclinic space group P-1 (no. 2). These complexes are dinuclear cluster structures which contain two lanthanide ions (Ln^{3+} , Ln1 and Ln2), six deprotonated IMBA and two dmp, forming an electroneutral unit (Fig. 1) [2]. In these complexes, IMBA has two coordination modes of bridge and chelation (Fig. 2). Ln–O and Ln–N bond lengths and bond angles are in line with the reported lanthanide complexes (Tables 1–3) [3–8]. PXRD of **1a** that incubation in aqueous solution for as long as the sensing time (1 h) was in line with the as-synthesized sample and calculated data, confirming that the sensor **1a** is a highly stable (Fig. 3) [9–11].

1.1. FT-IR spectra of 1a–1c

FT-IR spectra of **1a–1c** (Fig. 4) are similar at 1710–1430 cm^{-1} and are assigned to C=O, C–C and C=C vibrations of the IMBA and dmp [12,13]. The bands assignment at 1000–1300 cm^{-1} is difficult

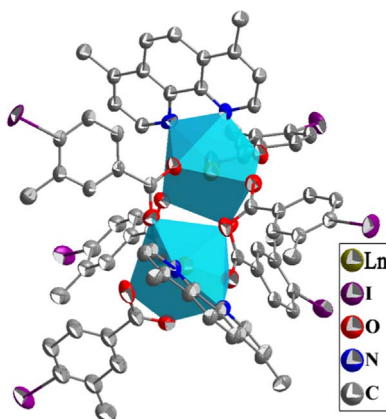


Fig. 1. The dinuclear cluster structure.

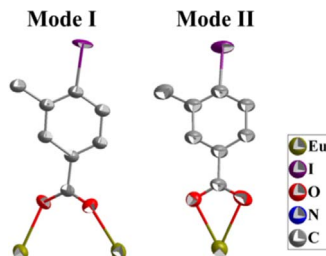


Fig. 2. Coordination modes of the ligand IMBA in 1a–1c.

Table 1

Selected bond lengths and bond angles of 1a.

Eu(1)–O(3)	2.319(6)	Eu(2)–O(6)	2.313(5)
Eu(1)–O(9)	2.350(5)	Eu(2)–O(8)	2.353(6)
Eu(1)–O(7)	2.367(6)	Eu(2)–O(10)	2.377(5)
Eu(1)–O(5)	2.376(6)	Eu(2)–O(4)	2.405(6)
Eu(1)–O(2)	2.432(6)	Eu(2)–O(12)	2.435(6)
Eu(1)–O(1)	2.439(6)	Eu(2)–O(11)	2.487(6)
Eu(1)–N(2)	2.600(7)	Eu(2)–N(4)	2.597(6)
Eu(1)–N(1)	2.629(7)	Eu(2)–N(3)	2.615(7)
Eu(1)–Eu(2)	4.2697(6)		
O(3)–Eu(1)–O(9)	74.2(2)	O(6)–Eu(2)–O(8)	78.3(2)
O(3)–Eu(1)–O(7)	116.2(2)	O(6)–Eu(2)–O(10)	117.1(2)
O(9)–Eu(1)–O(7)	77.1(2)	O(8)–Eu(2)–O(10)	77.4(2)
O(3)–Eu(1)–O(5)	76.7(2)	O(6)–Eu(2)–O(4)	80.1(2)
O(9)–Eu(1)–O(5)	133.8(2)	O(8)–Eu(2)–O(4)	134.0(2)
O(7)–Eu(1)–O(5)	84.7(2)	O(10)–Eu(2)–O(4)	77.2(2)
O(3)–Eu(1)–O(2)	83.6(2)	O(6)–Eu(2)–O(12)	153.0(2)
O(9)–Eu(1)–O(2)	76.5(2)	O(8)–Eu(2)–O(12)	128.6(2)
O(7)–Eu(1)–O(2)	140.7(2)	O(10)–Eu(2)–O(12)	75.9(2)
O(5)–Eu(1)–O(2)	134.3(2)	O(4)–Eu(2)–O(12)	80.2(2)
O(3)–Eu(1)–O(1)	83.9(2)	O(6)–Eu(2)–O(11)	149.9(2)
O(9)–Eu(1)–O(1)	127.5(2)	O(8)–Eu(2)–O(11)	78.2(2)
O(7)–Eu(1)–O(1)	153.3(2)	O(10)–Eu(2)–O(11)	75.3(2)
O(5)–Eu(1)–O(1)	83.3(2)	O(4)–Eu(2)–O(11)	129.9(2)
O(2)–Eu(1)–O(1)	53.7(2)	O(12)–Eu(2)–O(11)	53.0(2)
O(3)–Eu(1)–N(2)	147.7(2)	O(6)–Eu(2)–N(4)	82.8(2)
O(9)–Eu(1)–N(2)	77.8(2)	O(8)–Eu(2)–N(4)	137.9(2)
O(7)–Eu(1)–N(2)	72.0(2)	O(10)–Eu(2)–N(4)	144.2(2)
O(5)–Eu(1)–N(2)	135.4(2)	O(4)–Eu(2)–N(4)	77.7(2)
O(2)–Eu(1)–N(2)	74.3(2)	O(12)–Eu(2)–N(4)	75.1(2)
O(1)–Eu(1)–N(2)	100.9(2)	O(11)–Eu(2)–N(4)	102.6(2)
O(3)–Eu(1)–N(1)	148.8(2)	O(6)–Eu(2)–N(3)	80.1(2)
O(9)–Eu(1)–N(1)	136.5(2)	O(8)–Eu(2)–N(3)	77.1(2)
O(7)–Eu(1)–N(1)	75.2(2)	O(10)–Eu(2)–N(3)	145.1(2)
O(5)–Eu(1)–N(1)	75.6(2)	O(4)–Eu(2)–N(3)	137.5(2)
O(2)–Eu(1)–N(1)	106.0(2)	O(12)–Eu(2)–N(3)	102.6(2)
O(1)–Eu(1)–N(1)	78.8(2)	O(11)–Eu(2)–N(3)	76.5(2)
N(2)–Eu(1)–N(1)	62.1(2)	N(4)–Eu(2)–N(3)	62.7(2)

because of overlap [14,15]. The coordination of carboxyl with Ln^{3+} is confirmed by the FT-IR: the stretching vibration of $\text{C}=\text{O}$ decreases from 1647 to 1605 cm^{-1} and that of carboxyl $\text{O}-\text{H}$ at 3400 cm^{-1} disappears.

$[\text{Eu}_2(\text{IMBA})_6(\text{dmp})_2] \cdot (1\text{a})$. Yield: 37% based on Eu^{3+} . Anal. Calcd (%): C, 39.92; H, 2.645. Found (%): C, 40.13; H, 2.633. FT-IR (Fig. 4) (KBr pellet, cm^{-1}): 3450 (m), 2947 (w), 1620 (s), 1584 (w), 1438 (s), 1403 (m), 1305 (m), 1193 (w), 1033 (m), 934 (w), 872 (m), 789 (s), 747 (w), 550 (w), 482 (w).

Table 2
Selected bond lengths and bond angles of **1b**.

Gd(1)–O(7)	2.306(5)	Gd(2)–O(10)	2.308(5)
Gd(1)–O(5)	2.341(5)	Gd(2)–O(4)	2.339(5)
Gd(1)–O(3)	2.367(5)	Gd(2)–O(6)	2.362(5)
Gd(1)–O(9)	2.380(5)	Gd(2)–O(8)	2.371(5)
Gd(1)–O(1)	2.437(5)	Gd(2)–O(11)	2.430(5)
Gd(1)–O(2)	2.488(5)	Gd(2)–O(12)	2.437(5)
Gd(1)–N(1)	2.588(6)	Gd(2)–N(4)	2.585(6)
Gd(1)–N(2)	2.591(6)	Gd(2)–N(3)	2.609(6)
O(7)–Gd(1)–O(5)	78.65(18)	O(10)–Gd(2)–O(4)	74.41(18)
O(7)–Gd(1)–O(3)	117.31(18)	O(10)–Gd(2)–O(6)	116.16(18)
O(5)–Gd(1)–O(3)	76.83(18)	O(4)–Gd(2)–O(6)	77.10(17)
O(7)–Gd(1)–O(9)	80.21(19)	O(10)–Gd(2)–O(8)	76.62(18)
O(5)–Gd(1)–O(9)	133.41(18)	O(4)–Gd(2)–O(8)	133.46(17)
O(3)–Gd(1)–O(9)	76.91(18)	O(6)–Gd(2)–O(8)	84.11(18)
O(7)–Gd(1)–O(1)	153.13(18)	O(10)–Gd(2)–O(11)	83.79(19)
O(5)–Gd(1)–O(1)	128.19(18)	O(4)–Gd(2)–O(11)	127.74(17)
O(3)–Gd(1)–O(1)	75.70(17)	O(6)–Gd(2)–O(11)	153.21(17)
O(9)–Gd(1)–O(1)	80.34(19)	O(8)–Gd(2)–O(11)	83.52(18)
O(7)–Gd(1)–O(2)	149.98(18)	O(10)–Gd(2)–O(12)	83.41(19)
O(5)–Gd(1)–O(2)	78.04(19)	O(4)–Gd(2)–O(12)	76.68(18)
O(3)–Gd(1)–O(2)	75.05(18)	O(6)–Gd(2)–O(12)	141.09(17)
O(9)–Gd(1)–O(2)	129.78(18)	O(8)–Gd(2)–O(12)	134.53(18)
O(1)–Gd(1)–O(2)	52.80(18)	O(11)–Gd(2)–O(12)	53.70(17)
O(7)–Gd(1)–N(1)	82.55(18)	O(10)–Gd(2)–N(4)	147.67(19)
O(5)–Gd(1)–N(1)	138.21(18)	O(4)–Gd(2)–N(4)	77.76(18)
O(3)–Gd(1)–N(1)	144.50(18)	O(6)–Gd(2)–N(4)	72.34(19)
O(9)–Gd(1)–N(1)	78.24(18)	O(8)–Gd(2)–N(4)	135.53(18)
O(1)–Gd(1)–N(1)	75.46(18)	O(11)–Gd(2)–N(4)	100.84(19)
O(2)–Gd(1)–N(1)	102.84(19)	O(12)–Gd(2)–N(4)	74.37(19)
O(7)–Gd(1)–N(2)	80.26(19)	O(10)–Gd(2)–N(3)	148.29(19)
O(5)–Gd(1)–N(2)	77.39(18)	O(4)–Gd(2)–N(3)	136.91(17)
O(3)–Gd(1)–N(2)	144.74(18)	O(6)–Gd(2)–N(3)	75.63(18)
O(9)–Gd(1)–N(2)	138.15(18)	O(8)–Gd(2)–N(3)	75.54(18)
O(1)–Gd(1)–N(2)	102.57(19)	O(11)–Gd(2)–N(3)	78.30(18)
O(2)–Gd(1)–N(2)	76.40(18)	O(12)–Gd(2)–N(3)	105.88(19)
N(1)–Gd(1)–N(2)	62.76(18)	N(4)–Gd(2)–N(3)	62.50(18)

Table 3
Selected bond lengths and bond angles of **1c**.

Tb(1)–O(10)	2.288(4)	Tb(2)–O(6)	2.295(4)
Tb(1)–O(12)	2.322(4)	Tb(2)–O(3)	2.333(4)
Tb(1)–O(4)	2.344(4)	Tb(2)–O(11)	2.340(4)
Tb(1)–O(5)	2.360(4)	Tb(2)–O(9)	2.351(4)
Tb(1)–O(2)	2.422(4)	Tb(2)–O(7)	2.414(4)
Tb(1)–O(1)	2.478(4)	Tb(2)–O(8)	2.419(4)
Tb(1)–N(4)	2.563(5)	Tb(2)–N(1)	2.566(5)
Tb(1)–N(3)	2.579(5)	Tb(2)–N(2)	2.592(5)
O(10)–Tb(1)–O(12)	78.92(15)	O(6)–Tb(2)–O(3)	74.49(15)
O(10)–Tb(1)–O(4)	117.29(14)	O(6)–Tb(2)–O(11)	116.18(15)
O(12)–Tb(1)–O(4)	76.57(15)	O(3)–Tb(2)–O(11)	77.18(15)
O(10)–Tb(1)–O(5)	79.82(16)	O(6)–Tb(2)–O(9)	76.61(16)
O(12)–Tb(1)–O(5)	133.23(15)	O(3)–Tb(2)–O(9)	133.03(14)
O(4)–Tb(1)–O(5)	77.10(15)	O(11)–Tb(2)–O(9)	83.50(15)
O(10)–Tb(1)–O(2)	152.67(15)	O(6)–Tb(2)–O(7)	83.26(16)
O(12)–Tb(1)–O(2)	128.38(15)	O(3)–Tb(2)–O(7)	128.16(15)
O(4)–Tb(1)–O(2)	75.99(14)	O(11)–Tb(2)–O(7)	153.06(15)
O(5)–Tb(1)–O(2)	80.40(16)	O(9)–Tb(2)–O(7)	83.32(15)
O(10)–Tb(1)–O(1)	149.68(16)	O(6)–Tb(2)–O(8)	82.95(16)
O(12)–Tb(1)–O(1)	77.54(16)	O(3)–Tb(2)–O(8)	76.69(15)
O(4)–Tb(1)–O(1)	75.13(15)	O(11)–Tb(2)–O(8)	141.55(14)

Table 3 (continued)

O(5)–Tb(1)–O(1)	130.47(16)	O(9)–Tb(2)–O(8)	134.75(15)
O(2)–Tb(1)–O(1)	53.52(16)	O(7)–Tb(2)–O(8)	54.21(14)
O(10)–Tb(1)–N(4)	82.34(15)	O(6)–Tb(2)–N(1)	147.45(17)
O(12)–Tb(1)–N(4)	138.72(15)	O(3)–Tb(2)–N(1)	77.72(16)
O(4)–Tb(1)–N(4)	144.31(16)	O(11)–Tb(2)–N(1)	72.84(15)
O(5)–Tb(1)–N(4)	77.77(15)	O(9)–Tb(2)–N(1)	135.77(16)
O(2)–Tb(1)–N(4)	75.16(15)	O(7)–Tb(2)–N(1)	101.27(16)
O(1)–Tb(1)–N(4)	103.37(16)	O(8)–Tb(2)–N(1)	74.40(16)
O(10)–Tb(1)–N(3)	79.95(16)	O(6)–Tb(2)–N(2)	147.94(16)
O(12)–Tb(1)–N(3)	77.25(15)	O(3)–Tb(2)–N(2)	137.22(16)
O(4)–Tb(1)–N(3)	144.71(15)	O(11)–Tb(2)–N(2)	75.90(15)
O(5)–Tb(1)–N(3)	138.06(15)	O(9)–Tb(2)–N(2)	75.51(15)
O(2)–Tb(1)–N(3)	102.97(16)	O(7)–Tb(2)–N(2)	78.09(16)
O(1)–Tb(1)–N(3)	76.44(15)	O(8)–Tb(2)–N(2)	106.09(16)
N(4)–Tb(1)–N(3)	63.39(15)	N(1)–Tb(2)–N(2)	62.90(16)

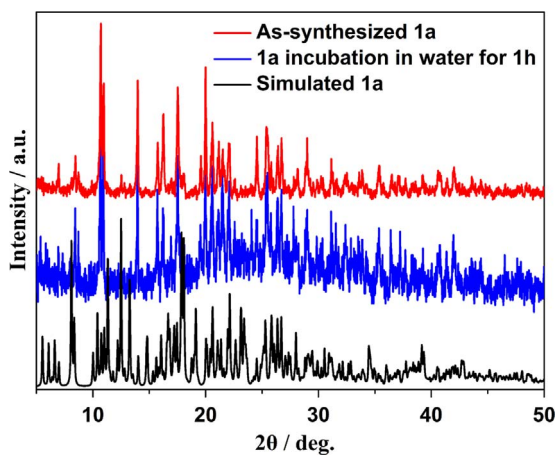


Fig. 3. PXRD patterns comparison of simulated **1a**, as-synthesized **1a** and bulk sample **1a** immersed in water for 1 h, these peaks compete with each other very well, confirming **1a** is a stable sensor.

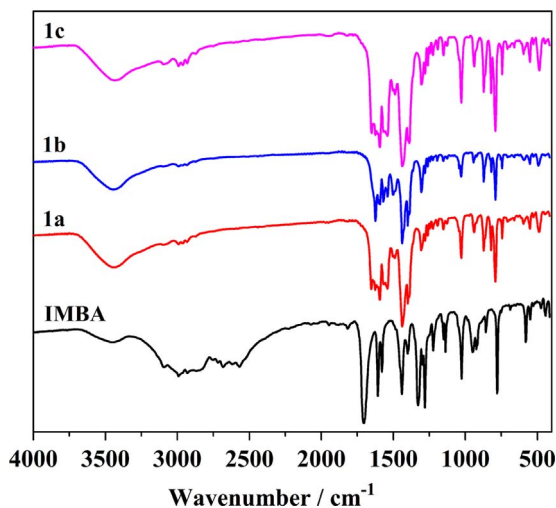


Fig. 4. FT-IR spectra of the ligand IMBA and as-synthesized **1a**–**1c**.

[Gd₂(IMBA)₆(dmp)₂] (1b). Yield: 34% based on Gd³⁺. Anal. Calcd (%): C, 39.74; H, 2.633. Found (%): C, 39.61; H, 2.618. FT-IR (Fig. 4) (KBr pellet, cm⁻¹): 3435 (m), 2995 (w), 1648 (w), 1592 (s), 1542 (m), 1495 (w), 1438 (s), 1305 (m), 1152 (w), 1033 (s), 943 (m), 872 (s), 789 (s), 739 (m), 600 (w), 550 (w), 488 (m).

[Tb₂(IMBA)₆(dmp)₂] (1c). Yield: 35% based on Tb³⁺. Anal. Calcd (%): C, 39.68; H, 2.629. Found (%): C, 39.79; H, 2.637. FT-IR (Fig. 4) (KBr pellet, cm⁻¹): 3443 (m), 2980 (w), 1627 (w), 1592 (s), 1542 (m), 1494 (w), 1430 (s), 1312 (w), 1152 (w), 1033 (s), 934 (w), 872 (m), 824 (m), 789 (s), 739 (w), 550 (w), 488 (w).

2. Experimental design, materials, and methods

Lanthanide complexes **1a–1c** were synthesized with solvothermal method by heating a mixture of Ln(NO₃)₃ · 6H₂O (Ln=Eu, Gd, Tb), dmp and IMBA at a molar ratio of 1:1:1.5 at 333 K for 120 h. The colorless block single crystals of **1a–1c** were collected by filtration, and mounted on a glass fiber [1].

Single crystal X-ray diffraction data were obtained on an instrument of Bruker SMART 1000 CCD, at wavelength of 0.71073 Å (Mo-Kα radiation) at 25 °C. The structures were refined by full-matrix least-squares methods with SHELXL-97 module. Phase purity of bulk samples were tested by PXRD, on a DMAX2200VPC diffractometer [7].

Acknowledgments

The authors also acknowledge the financial support of Jiangxi Normal University.

Transparency document. Supporting information

Transparency data associated with this article can be found in the online version at <https://doi.org/10.1016/j.dib.2018.09.063>.

References

- [1] Z.-P. Zhao, Y.-F. Jiang, Y. Chen, H.-R. Li, Y. Zheng, C.-H. Zeng, S. Zhong, Y.-L. Zhao, Highly luminescent lanthanide complexes as bifunctional sensor for Et₂O and Fe²⁺, *J. Lumin.* 204 (2018) 560–567.
- [2] Z.-P. Zhao, K. Zheng, H.-R. Li, C.-H. Zeng, S. Zhong, S.W. Ng, et al., Structure variation and luminescence of 3D, 2D and 1D lanthanide coordination polymers with 1,3-adamantanediicetic acid, *Inorg. Chim. Acta* 482 (2018) 340–346.
- [3] M.-Q. Yang, C.-P. Zhou, Y. Chen, J.-J. Li, C.-H. Zeng, S. Zhong, Highly sensitive and selective sensing of CH₃Hg⁺ via oscillation effect in Eu-cluster, *Sens. Actuators B Chem.* 248 (2017) 589–596.
- [4] C.-H. Zeng, H. Wu, Z. Luo, J. Yao, Weak interactions cause selective cocrystal formation of lanthanide nitrates and tetra-2-pyridinylpyrazine, *CrystEngComm* 20 (2018) 1123–1129.
- [5] K. Zheng, Z.-Q. Liu, Y. Huang, F. Chen, C.-H. Zeng, S. Zhong, et al., Highly luminescent Ln-MOFs based on 1,3-adamantanediicetic acid as bifunctional sensor, *Sens. Actuators B Chem.* 257 (2018) 705–713.
- [6] C.-H. Zeng, H.-R. Li, Z.-Q. Liu, F. Chen, S. Zhong, Structural data of thermostable 3D Ln-MOFs that based on flexible ligand of 1,3-adamantanediicetic acid, *Data Brief* 17 (2018) 689–697.
- [7] C.-H. Zeng, F.-L. Zhao, Y.-Y. Yang, M.-Y. Xie, X.-M. Ding, D.-J. Hou, et al., Unusual method for phenolic hydroxyl bridged lanthanide CPs: syntheses, characterization, one and two photon luminescence, *Dalton Trans.* 42 (2013) 2052–2061.
- [8] C.-H. Zeng, J.-L. Wang, Y.-Y. Yang, T.-S. Chu, S.-L. Zhong, S.W. Ng, et al., Lanthanide CPs: the guest-tunable drastic changes of luminescent quantum yields, and two photon luminescence, *J. Mater. Chem. C* 2 (2014) 2235–2242.
- [9] R.R. Su, P. Tao, Y. Han, C.H. Zeng, S.L. Zhong, Lanthanide coordination polymer nanosheet aggregates: solvothermal synthesis and downconversion luminescence, *J. Nanomater.* (2016).
- [10] P. Tao, C.-H. Zeng, K. Zheng, C.-Q. Huang, S.-L. Zhong, Uniform terbium coordination polymer microspheres: preparation and luminescence, *J. Inorg. Organomet. Polym. Mater.* 26 (2016) 1087–1094.
- [11] S.-S. Xu, P. Tao, C.-H. Zeng, Y. Wang, L.-F. Gao, Q.-Q. Nie, et al., Lanthanide-pamoate-frameworks: visible light excitation for NIR luminescence, *Inorg. Chim. Acta* 447 (2016) 92–97.
- [12] C.-H. Zeng, X.-T. Meng, S.-S. Xu, L.-J. Han, S. Zhong, M.-Y. Jia, A polymorphic lanthanide complex as selective Co²⁺ sensor and luminescent timer, *Sens. Actuators B Chem.* 221 (2015) 127–135.

- [13] Z.-Q. Yan, X.-T. Meng, R.-R. Su, C.-H. Zeng, Y.-Y. Yang, S. Zhong, et al., Basophilic method for lanthanide MOFs with a drug ligand: crystal structure and luminescence, *Inorg. Chim. Acta* 432 (2015) 41–45.
- [14] C.-H. Zeng, S. Xie, M. Yu, Y. Yang, X. Lu, Y. Tong, Facile synthesis of large-area CeO₂/ZnO nanotube arrays for enhanced photocatalytic hydrogen evolution, *J. Power Sources* 247 (2014) 545–550.
- [15] C.-H. Zeng, K. Zheng, K.-L. Lou, X.-T. Meng, Z.-Q. Yan, Z.-N. Ye, et al., Synthesis of porous europium oxide particles for photoelectrochemical water splitting, *Electrochim. Acta* 165 (2015) 396–401.